NASA TM X-272

TECHNICAL MEMORANDUM
X-272

STATIC LONGITUDINAL AND LATERAL STABILITY CHARACTERISTICS AT A MACH NUMBER OF 3.11 OF SQUARE AND CIRCULAR PLAN-FORM REENTRY VEHICLES, WITH SOME EFFECTS OF CONTROLS AND LEADING-EDGE EXTENSIONS

By Byron M. Jaquet

Langley Research Center
Langley Field, Va.

NATIONAL AERONAUTICS AND SPACE ADMINISTRATION

WASHINGTON May 1960

CONFIDENTIAL

NATIONAL AERONAUTICS AND SPACE ADMINISTRATION

TECHNICAL MEMORANDUM X-272

STATIC LONGITUDINAL AND LATERAL STABILITY CHARACTERISTICS AT A MACH NUMBER OF 3.11 OF SQUARE AND CIRCULAR PLAN-FORM REENTRY VEHICLES, WITH SOME EFFECTS OF CONTROLS AND LEADING-EDGE EXTENSIONS*

By Byron M. Jaquet

SUMMARY

An investigation was made at a Mach number of 3.11 to determine the static longitudinal and lateral stability characteristics and some control characteristics of a square plan-form reentry vehicle with leading-edge extensions and a circular plan-form reentry vehicle with pyramidal controls. The tests were made at Reynolds numbers per foot of 12.050×10^6 to 13.060×10^6 at angles of attack from approximately -5° to 13° and for two sideslip angles, 0° and 6°.

The square plan-form vehicle had static longitudinal stability about the quarter chord and extensions of the chord reduced the stability. An extension of the leading edge of one-fourth of the chord resulted in neutral static longitudinal stability. The directional stability of the square plan-form vehicle without extensions was essentially invariant with angle of attack. Extension of the leading edge somewhat reduced the directional stability.

For the circular plan-form vehicle, pyramidal controls located near the lower surface of the wing had greater control effectiveness than controls located above the wing surface. The lower controls, however, increased the already large negative pitching moments that existed at zero angle of attack whereas the upper controls decreased the pitching moment at zero angle of attack. The circular plan-form vehicle was directionally stable for the angle-of-attack range of the investigation.

*Title, Unclassified.

INTRODUCTION

The design of a vehicle suitable for reentry from orbital flight entails a compromise between the optimum configurations when heating, stability and control, range, and payload are considered. As a result, many different types of configurations have been considered. (See, for example, refs. 1 to 3.)

This paper presents, for a Mach number of 3.11, the static longitudinal and lateral stability and some control characteristics of two configurations which might be suitable for manned reentry. One configuration used in the present investigation was the variable-geometry type. It had a small fuselage located on the upper surface of a square plan-form wing. The fuselage nose coincided with the wing leading edge. The wing had an extendable leading edge which could be used to control the center-of-pressure location. Twin vertical tails were located at the wing tips and would be available for control when deflected from the vertical. The second configuration was circular in plan form with a flat bottom and had twin pyramidal controls which were tested in two positions. L 8 0 9

The investigation was made in the Mach number 3.11 jet of the Langley gas dynamics laboratory at Reynolds numbers per foot of 12.050×10^6 to 13.060×10^6 for angles of attack to 13° at two sideslip angles, 0° and 6°.

SYMBOLS

Data are referred to the axes system shown in figure 1. The coefficients of the square plan-form configuration are based on the area, span, and chord of the square plan-form wing without extensions and the moment center (fig. 2) is at 0.25 chord from the leading edge. All coefficients for the circular plan-form configuration are based on the area and diameter of the circle and are referred to the moment center indicated in figure 2.

b	span of square plan-form wing, ft
C_D'	approximate drag coefficient, $\frac{\text{Drag}}{qS}$
$C_{D,b}$	base drag coefficient, $\frac{\text{Base drag}}{qS}$

C_L lift coefficient, $\frac{\text{Lift}}{qS}$

C_l rolling-moment coefficient, $\frac{\text{Rolling moment}}{qS(b \text{ or } d)}$

ΔC_l incremental rolling-moment coefficient, $\frac{(\text{Increment in rolling moment})_{\Delta\beta\approx 6^\circ}}{qS(b \text{ or } d)}$

C_m pitching-moment coefficient, $\frac{\text{Pitching moment}}{qS(c \text{ or } d)}$

$C_{m_\alpha} = \left(\frac{\partial C_m}{\partial \alpha}\right)_{\alpha\approx 0}$

C_n yawing-moment coefficient, $\frac{\text{Yawing moment}}{qS(b \text{ or } d)}$

ΔC_n incremental yawing-moment coefficient, $\frac{(\text{Increment in yawing moment})_{\Delta\beta\approx 6^\circ}}{qS(b \text{ or } d)}$

C_Y side-force coefficient, $\frac{\text{Side force}}{qS}$

ΔC_Y incremental side-force coefficient, $\frac{(\text{Increment in side force})_{\Delta\beta\approx 6^\circ}}{qS}$

c chord of square plan-form wing, ft

d diameter of circular plan-form wing, ft

L/D lift-drag ratio

q dynamic pressure, lb/sq ft

S area of circular or square plan-form wing, sq ft

X longitudinal body axis

Y lateral body axis

Z	vertical body axis
α	angle of attack, deg
β	angle of sideslip, deg
$\Delta\beta$	incremental angle of sideslip, deg
δ	deflection of pyramidal controls from reference line, positive for nose up, deg

MODELS AND EQUIPMENT

The models used in this investigation were machined from stainless steel; their details are shown in figure 2. The square plan-form wing had a Clark Y airfoil section which was cut at 68.6-percent chord and had a fuselage on its upper surface extending rearward from the leading edge of the wing. This model is referred to hereinafter as the square model. The twin vertical tails of the square model had wedge airfoil sections. The circular plan-form wing was a spherical segment with a radius leading edge. The thickness at the center of the circle was 15.62 percent of the diameter. The pyramidal controls were positioned on supports at 0° and -20° deflection with respect to the flat bottom surface of the wing. A small fuselage at the rear of the wing provided coverage for the balance. This model is referred to as the circular model. Photographs of the models are presented as figure 3.

The models were tested in the Mach number 3.11 jet of the Langley gas dynamics laboratory. The test section of the jet was approximately 12 inches by 12.5 inches.

A six-component strain-gage balance was attached to a sting and the models were mounted on the balance. The sting was hydraulically driven through an angle-of-pitch range; a programmer provided a sequence of operation in which data were obtained at approximately 2° increments in pitch angle. A straight sting was used to obtain data at 0° sideslip and a sting bent 6° was used to obtain data at a sideslip angle of 6°. The angles of pitch and bend of the sting were resolved into angles of attack and sideslip in order to present data about the body axes.

When the tunnel was started, very large loads existed in the test section; therefore, it was necessary to use model holders to prevent balance damage. These are shown in figure 3(a) and were driven into a firm position on the model by a 90-pound-per-square-inch air supply. A valve and tripping arrangement permitted the model holders to be retracted after the tunnel was started.

TESTS AND CORRECTIONS

The tests consisted of the measurement of normal force, axial force, side force, pitching moment, yawing moment, and rolling moment through an angle-of-attack range from approximately -5° to 13° at two sideslip angles, 0° and 6°. The maximum angle of attack varied with the configuration on account of the measured loads being at or near the balance design loads. All tests were made at a stagnation temperature of 100° F and at stagnation pressures from 70- to 77-pound-per-square-inch gage with resulting Reynolds numbers per foot from 12.050×10^6 to 13.060×10^6.

Before the axial forces were resolved into drag forces they were adjusted to correspond to the free-stream static pressure by using base pressures that were measured within the fuselage.

The angles of attack and sideslip were corrected for deflection of the balance and sting under load.

RESULTS AND DISCUSSION

Square Model

The square model was proposed as a configuration for which the center-of-pressure shift with Mach number could be controlled to desired limits by use of a controllable leading-edge extension. Longitudinal and lateral control and trimming would be provided by deflection of the twin vertical tails (fig. 2(a)); thus, the dihedral of the tails would be variable. Data presented herein are only for the case of 90° dihedral. All coefficient data are based on the dimensions of the model without leading-edge extensions.

Static longitudinal characteristics.- The variation of pitching-moment coefficient with angle of attack is presented in figure 4(a) for the square model without and with leading-edge extensions up to 50 percent of the reference chord. These data indicate large changes in static longitudinal stability with an increase in the leading-edge extension. This change in stability results from the shift in center of pressure from about 40 percent of the reference chord behind the moment reference for the model with the fully retracted extensions to about 13 percent of the reference chord ahead of the moment reference for the model with the maximum extension. For the Mach number of the test (3.11), extensions up to 25 percent of the reference chord could be used before the configuration would become unstable. Changes in vertical-tail dihedral angle could

have an appreciable effect on the stability; however, the tunnel to model size restrictions prevented testing the model with dihedral angles of the tail other than 90°. Differences in stability with the vertical tails on and off are the result of differences in drag of the configurations.

Lift and drag characteristics.- The lift and drag characteristics of the square model are presented in figure 4(b) for vertical tails on and in figure 4(c) for vertical tails off.

Maximum lift and maximum lift-drag ratio were not attained for the angle-of-attack range of the investigation. The large changes in lift coefficient due to the leading-edge extensions are primarily a result of the fact that these coefficients are based on the dimensions of the model with fully retracted extensions. When based on individual areas, the changes in lift coefficient due to the extensions are small. The lift-drag ratio, of course, is not affected by the reference area.

Static lateral characteristics.- The static lateral characteristics (fig. 5) were determined from the parameters $\Delta C_n/\Delta\beta$, $\Delta C_l/\Delta\beta$, and $\Delta C_Y/\Delta\beta$, which are increments in the respective coefficients due to approximately 6° increment in sideslip divided by the sideslip increment. Nonlinear variations of the coefficients with sideslip angle may exist, particularly at the higher angles of attack, and therefore the data presented herein may not be truly representative of the more conventional derivatives determined through $\beta = 0^\circ$ by taking slopes of coefficients determined at several sideslip angles.

The directional stability, as indicated by the parameter $\Delta C_n/\Delta\beta$, of the square model with the vertical tails on and with fully retracted extensions (fig. 5) is essentially invariant with angle of attack. Extension of the leading edge somewhat reduces the directional stability. With the tails off, the square model is directionally stable or neutrally stable for the angle-of-attack range of the investigation - probably the result of a stable contribution of the fuselage which is almost entirely behind the moment center (fig. 2(a)).

The value of $\Delta C_l/\Delta\beta$ is small for the square model with and without the tails, and the leading-edge extensions generally result in more negative slopes of $\Delta C_l/\Delta\beta$ with α.

Circular Model

Static longitudinal characteristics.- The variation of C_m with α for the circular model is shown in figure 6(a) for configurations with

upper controls (also for the model inverted without controls) and in figure 6(b) for configurations with lower controls. The data are referred to a moment center which provides $C_{m_\alpha} \approx 0$ at angles of attack near 0° for the wing alone. The tail length for the lower controls was about twice that for the upper controls. (See fig. 2(b).) An indication of the effect of the control supports on the stability characteristics is also shown in figure 6.

The upper controls at $\delta = 0^\circ$ (fig. 6(a)) produce positive pitching moments which tend to reduce the large negative value of C_m at $\alpha = 0^\circ$ of the wing alone and thus there is less pitching moment to be trimmed out by the deflection of the controls. The lower controls at $\delta = 0^\circ$ (fig. 6(b)) produce an opposite change in C_m at $\alpha = 0^\circ$, and thereby this effect increases the amount of control deflection required to trim out the large negative pitching moments. Even when the difference in tail length between the upper and lower controls is considered, the lower controls have greater effectiveness - particularly at positive angles of attack where the lower controls operate in a high dynamic-pressure region. Greater effectiveness would be obtained for the pyramidal controls at higher Mach numbers on the basis of reference 4 and, of course, less effectiveness would be obtained at lower Mach numbers so that a larger or a supplementary control would be required.

Configurations with the upper controls (fig. 6(a)) have static longitudinal stability for the angle-of-attack range of the investigation whereas configurations with the lower controls (fig. 6(b)) have neutral stability in the lower angle-of-attack range.

On the basis of linear control effectiveness at $\alpha = 0^\circ$, the upper and lower controls would have to be deflected on the order of -60° to trim at any appreciable angle of attack.

The circular wing alone, when inverted, has considerably more stability at the higher angles of attack than the flat-bottom configuration; in part, this may be caused by the contribution of the cylindrical afterbody, the axial force of which is acting below the moment reference point to produce a negative pitching moment.

Lift and drag characteristics.- Lift and drag characteristics of the circular model are presented in figure 7(a) for configurations with the upper controls and in figure 7(b) for configurations with the lower controls. As was the case with the square model, maximum lift and maximum lift-drag ratio were not achieved. With controls deflected -20°, the upper- and lower-control configurations have essentially the same lift-drag ratio at the highest angle of attack.

When compared with the flat-bottom model, the lift-drag ratio of the inverted (flat top) model (fig. 7(a)) increases more slowly with an increase in angle of attack because of a rapid increase in drag with increasing angle of attack for the inverted model.

As a result of lower drag, the square model had a higher value of L/D (fig. 4(b)) at the maximum angle of attack than the circular model (fig. 7(a)).

Static lateral characteristics.- The static lateral stability characteristics of the circular model are presented in figure 8. With the controls and supports off, the wing alone has directional stability as indicated by positive values of $\Delta C_n/\Delta\beta$. This result is probably due to the stable contribution of the cylindrical afterbody.

With the upper controls deflected -20°, the value of $\Delta C_n/\Delta\beta$ decreases slightly with an increase in angle of attack. With the lower controls deflected -20°, there is a larger variation of $\Delta C_n/\Delta\beta$ with angle of attack. The larger values of $\Delta C_n/\Delta\beta$ for the lower-control configurations than for the upper-control configurations result from the longer tail length of the lower-control configurations.

The upper controls have a greater effect on $\Delta C_l/\Delta\beta$ than the lower controls, but both the upper and lower controls when deflected -20° produce about the same values of $\Delta C_l/\Delta\beta$ at the higher angles of attack.

CONCLUSIONS

A wind-tunnel investigation was made at a Mach number of 3.11 to determine the static longitudinal and lateral characteristics and some control characteristics of a square plan-form reentry vehicle with leading-edge extensions and a circular plan-form vehicle with pyramidal controls for angles of attack from about -5° to 13° and at two sideslip angles, 0° and 6°. The results lead to the following conclusions:

1. The square plan-form vehicle had static longitudinal stability about the quarter chord and extensions of the chord reduced the stability. An extension of the leading edge of one-fourth of the reference chord resulted in neutral static longitudinal stability. The directional stability of the square plan-form vehicle without extensions was essentially invariant with angle of attack. Extension of the leading edge somewhat reduced the directional stability.

2. For the circular plan-form vehicle, pyramidal controls located near the lower surface of the wing had greater control effectiveness than controls located above the wing surface. The lower controls, however, increased the already large negative pitching moments that existed at zero angle of attack whereas the upper controls decreased the pitching moment at zero angle of attack. The circular plan-form vehicle was directionally stable for the angle-of-attack range of the investigation.

Langley Research Center,
National Aeronautics and Space Administration,
Langley Field, Va., January 19, 1960.

REFERENCES

1. Staff of Langley Flight Research Division (Compiled by Donald C. Cheatham): A Concept of a Manned Satellite Reentry Which is Completed With a Glide Landing. NASA TM X-226, 1959.

2. Cooper, Morton, and Gunn, Charles R.: Pressure Measurements on a Hypersonic Glide Configuration Having 79.5° Sweepback and 45° Dihedral at a Mach Number of 4.95. NASA TM X-223, 1959.

3. Ferri, Antonio, Feldman, Lewis, and Daskin, Walter: The Use of Lift for Re-entry From Satellite Trajectories. Jet Propulsion, vol. 27, no. 11, Nov. 1957, pp. 1184-1191.

4. Love, Eugene S.: The Use of Cones as Stabilizing and Control Surfaces at Hypersonic Speeds. NACA RM L57F14, 1957.

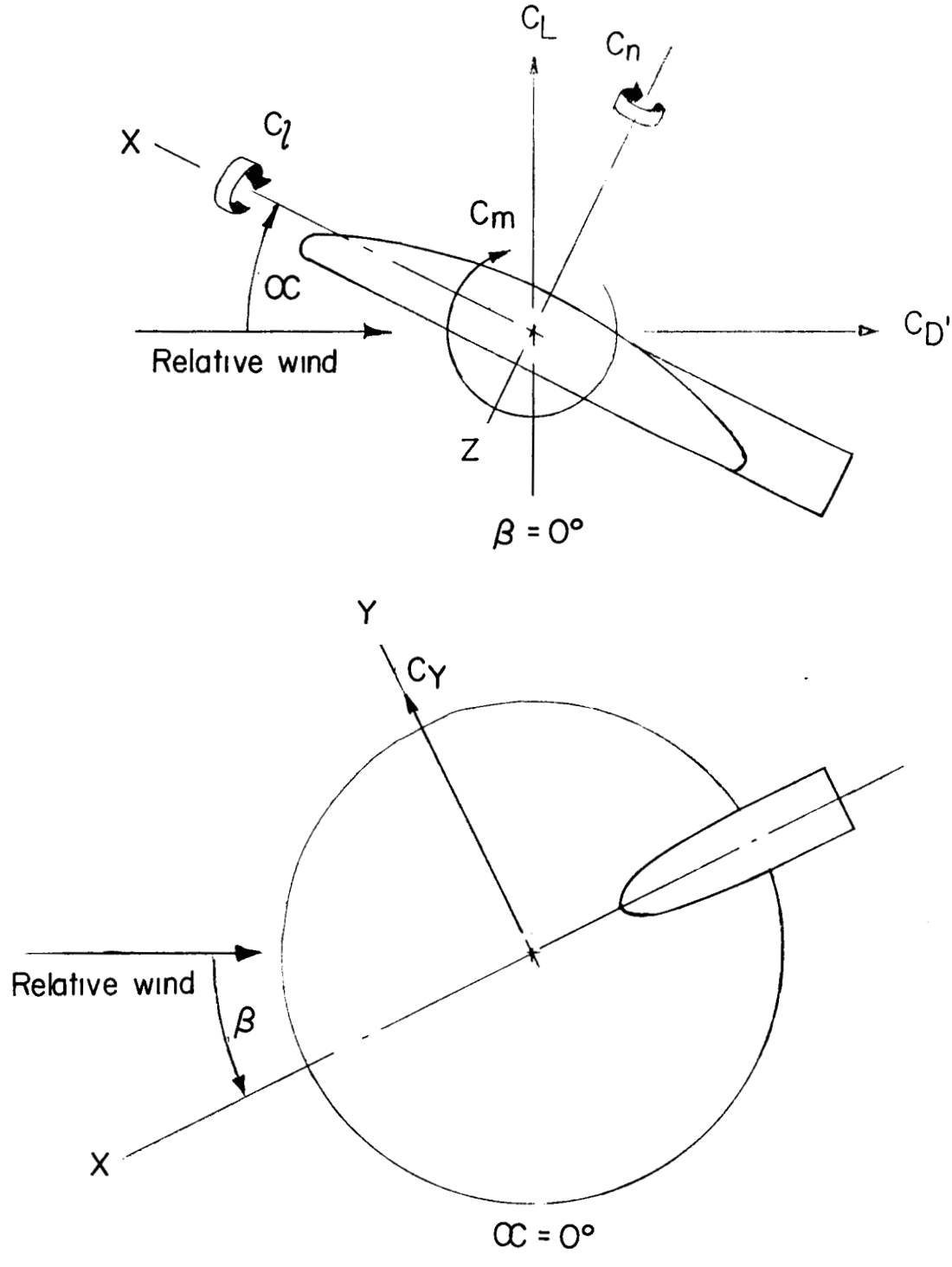

Figure 1.- System of axes. Arrows indicate positive directions of coefficients and angles.

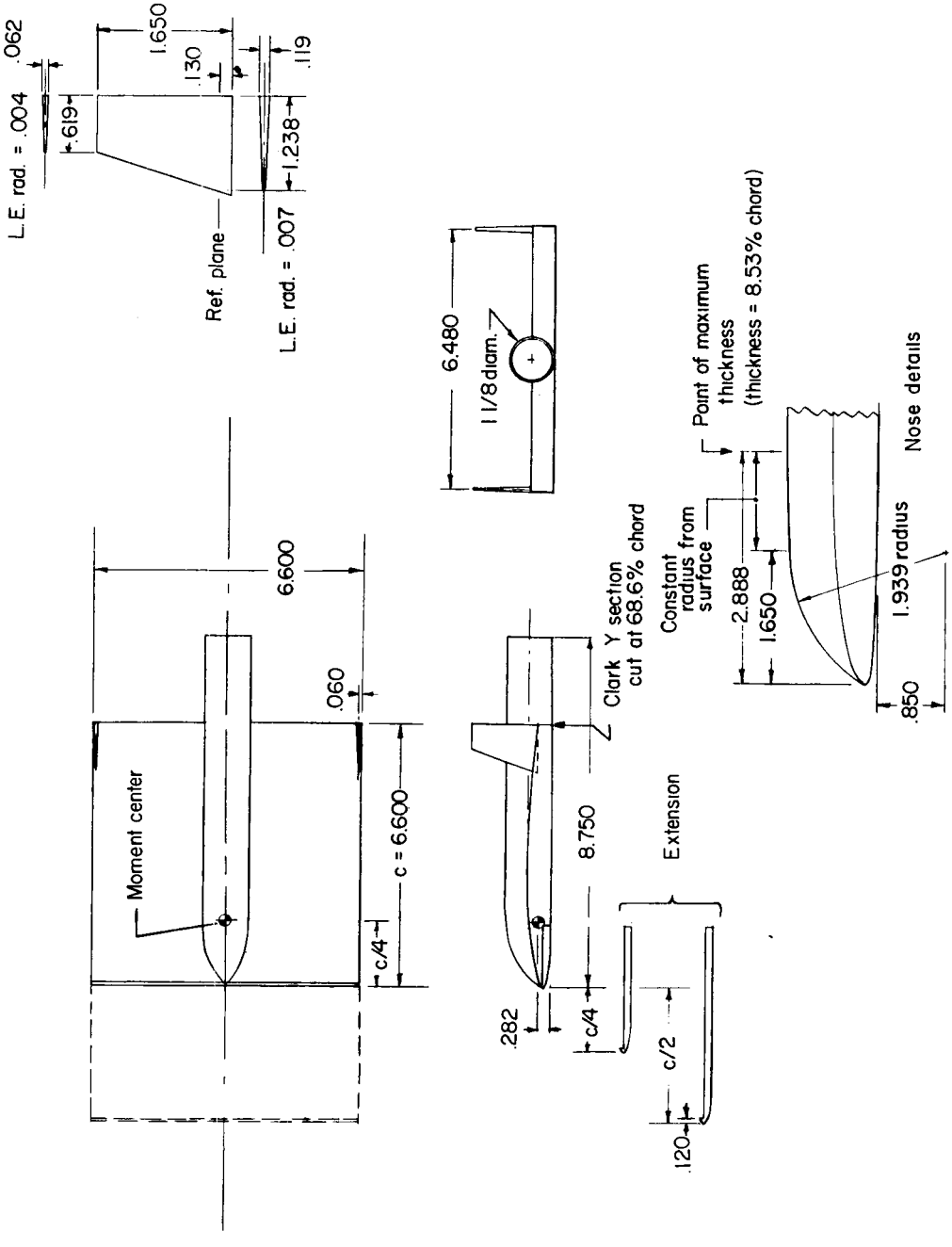

(a) Square model with extensions.

Figure 2.- Geometric details of models. All dimensions are in inches.

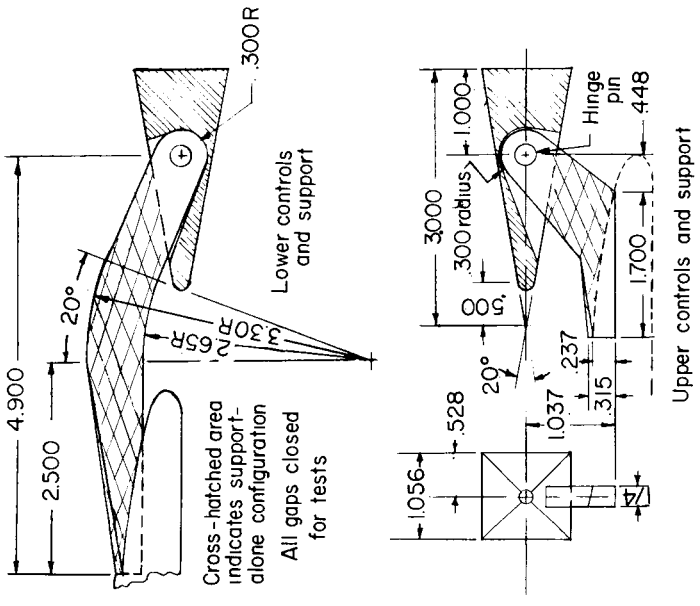

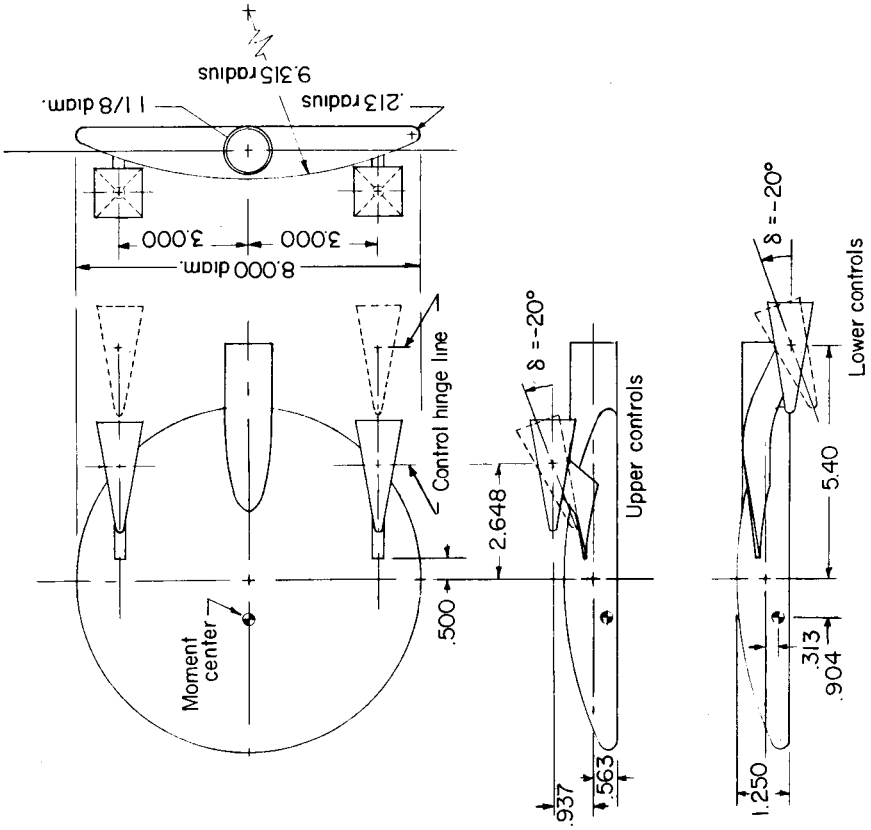

(b) Circular model.

Figure 2.- Concluded.

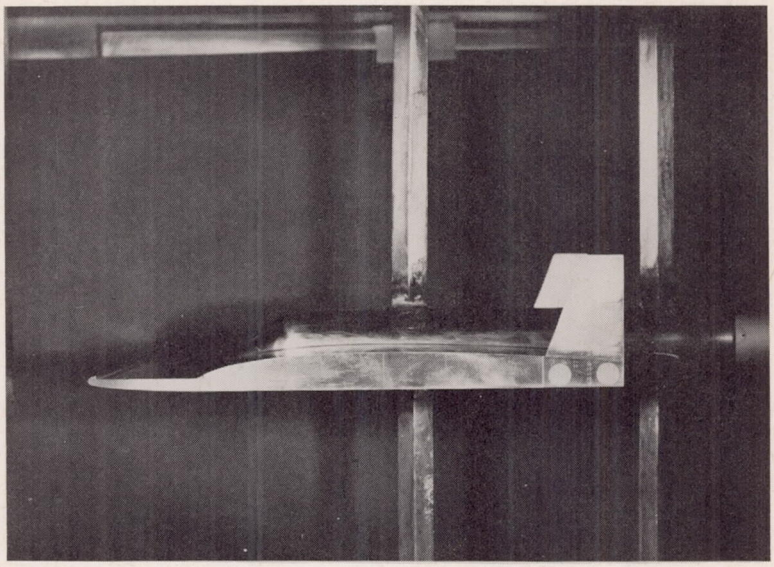

L-58-4351

(a) Square model with 25 percent chord-extensions. Model holders in position.

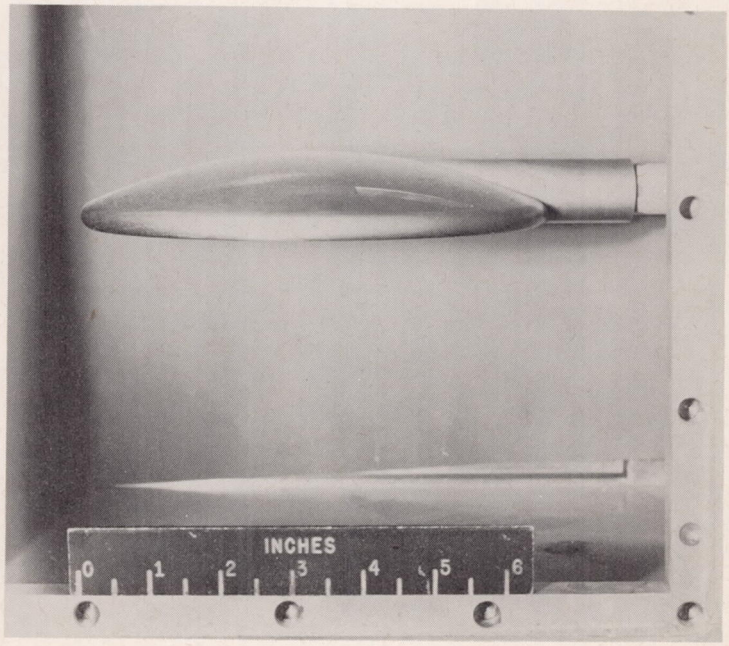

(b) Circular model. L-58-298a

Figure 3.- Photographs of models in test section.

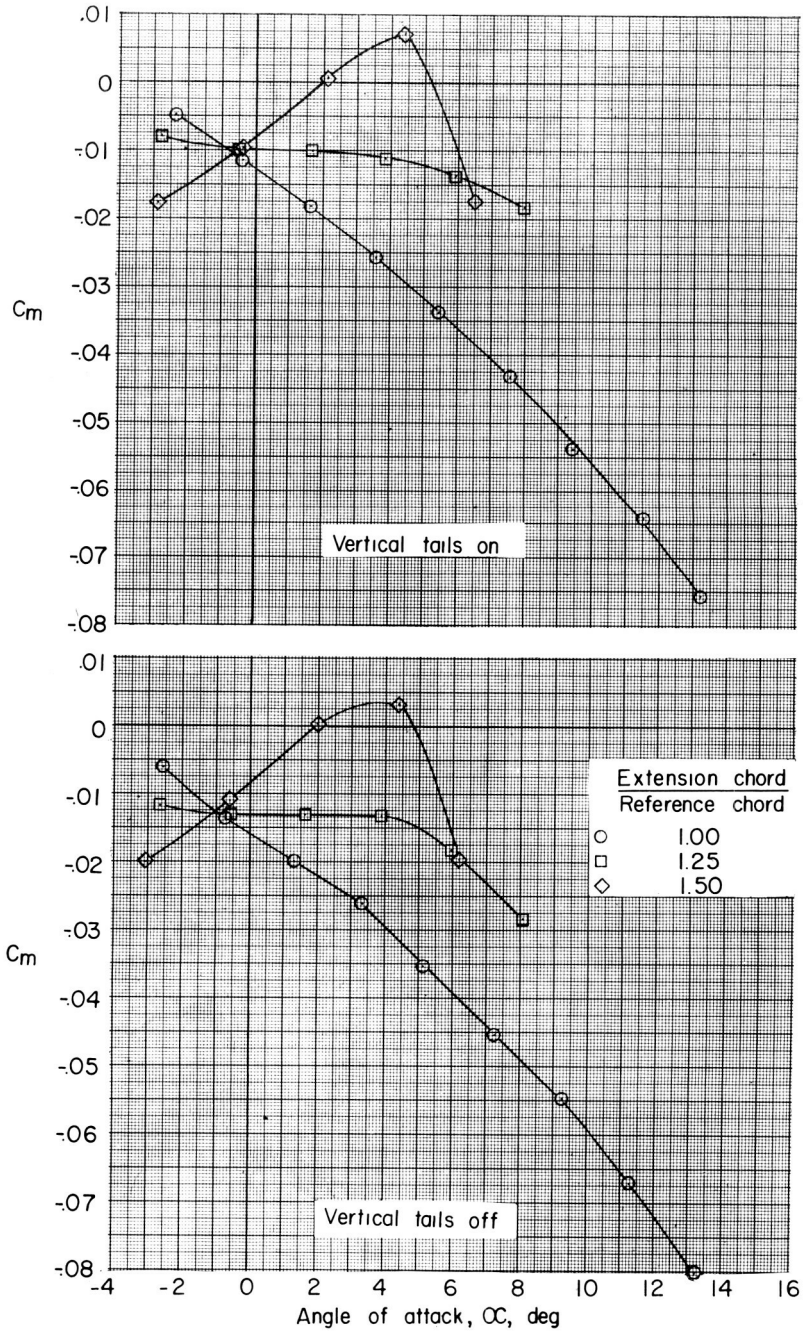

(a) Pitching-moment characteristics.

Figure 4.- Aerodynamic characteristics at 0^{o} sideslip of a square planform reentry vehicle with various leading-edge extensions.

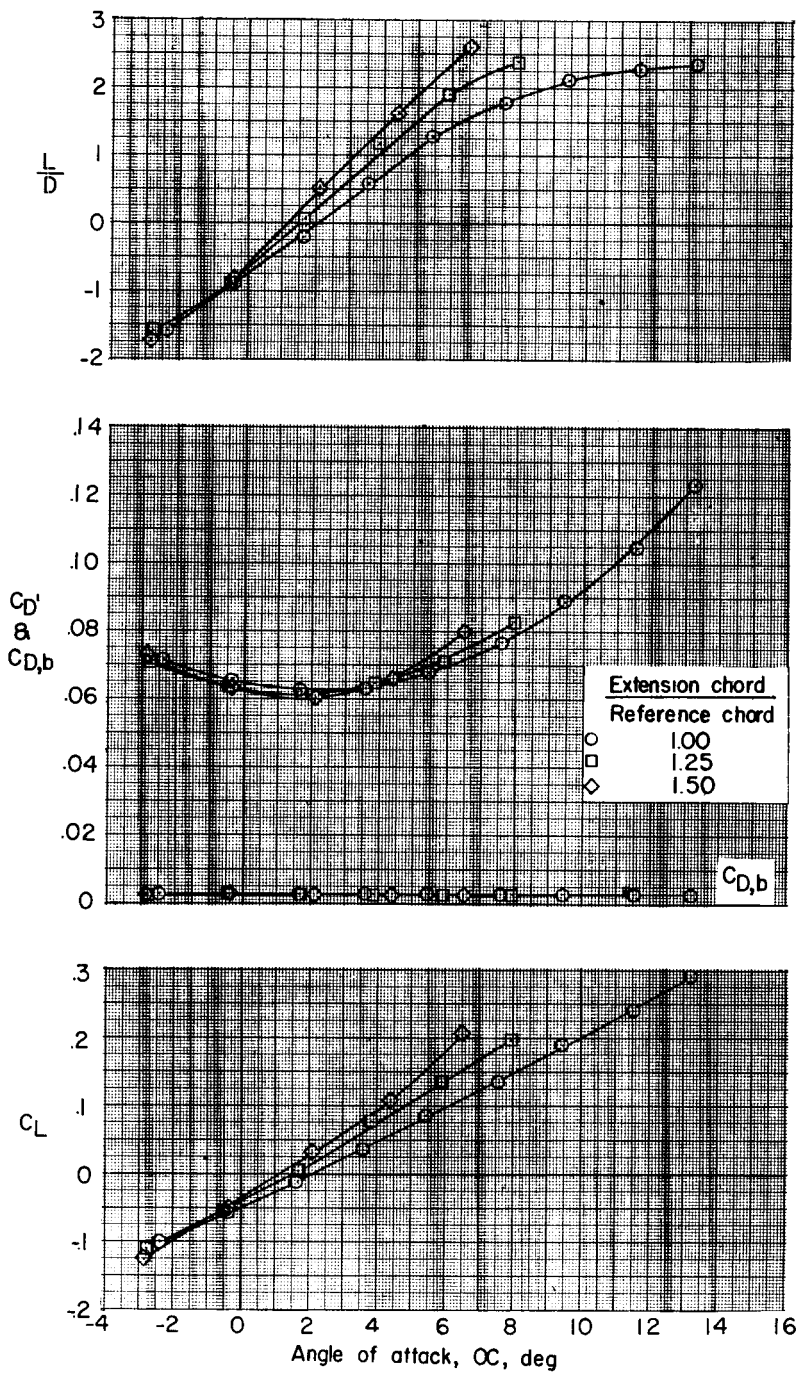

(b) Lift and drag characteristics. Vertical tails on.

Figure 4.- Continued.

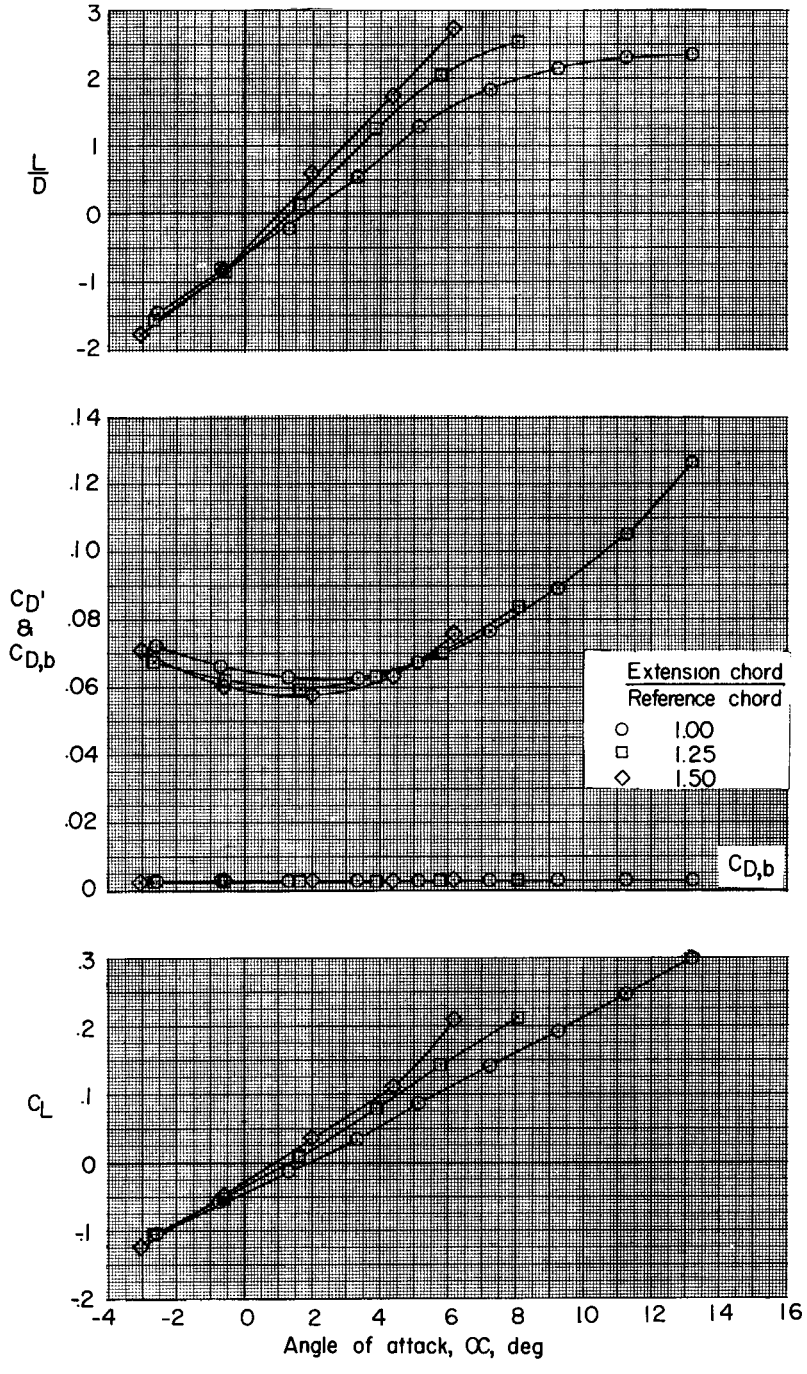

(c) Lift and drag characteristics. Vertical tails off.

Figure 4.- Concluded.

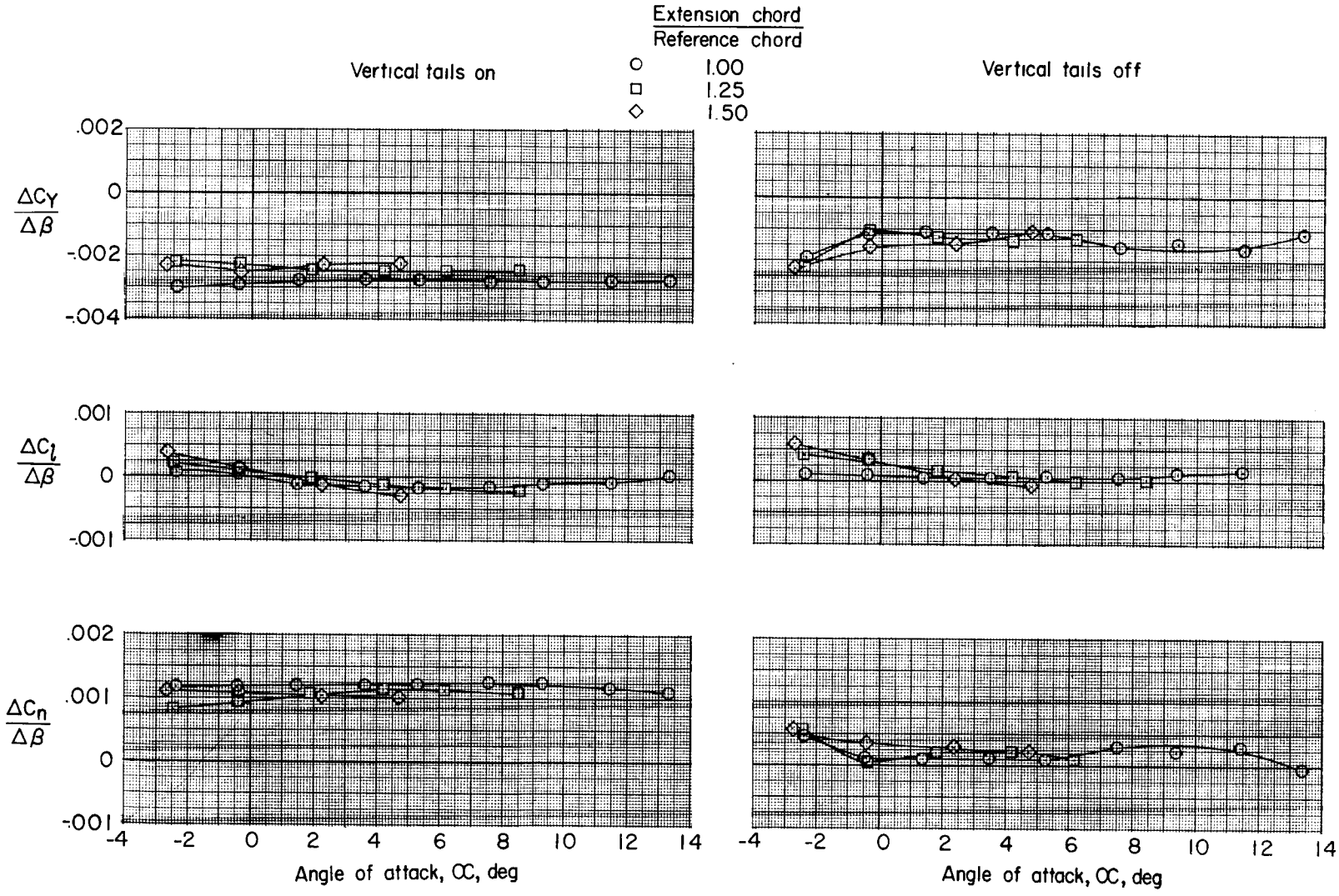

Figure 5.- Variation of $\Delta C_Y/\Delta\beta$, $\Delta C_l/\Delta\beta$, and $\Delta C_n/\Delta\beta$ with angle of attack for a square planform reentry vehicle with various leading-edge extensions.

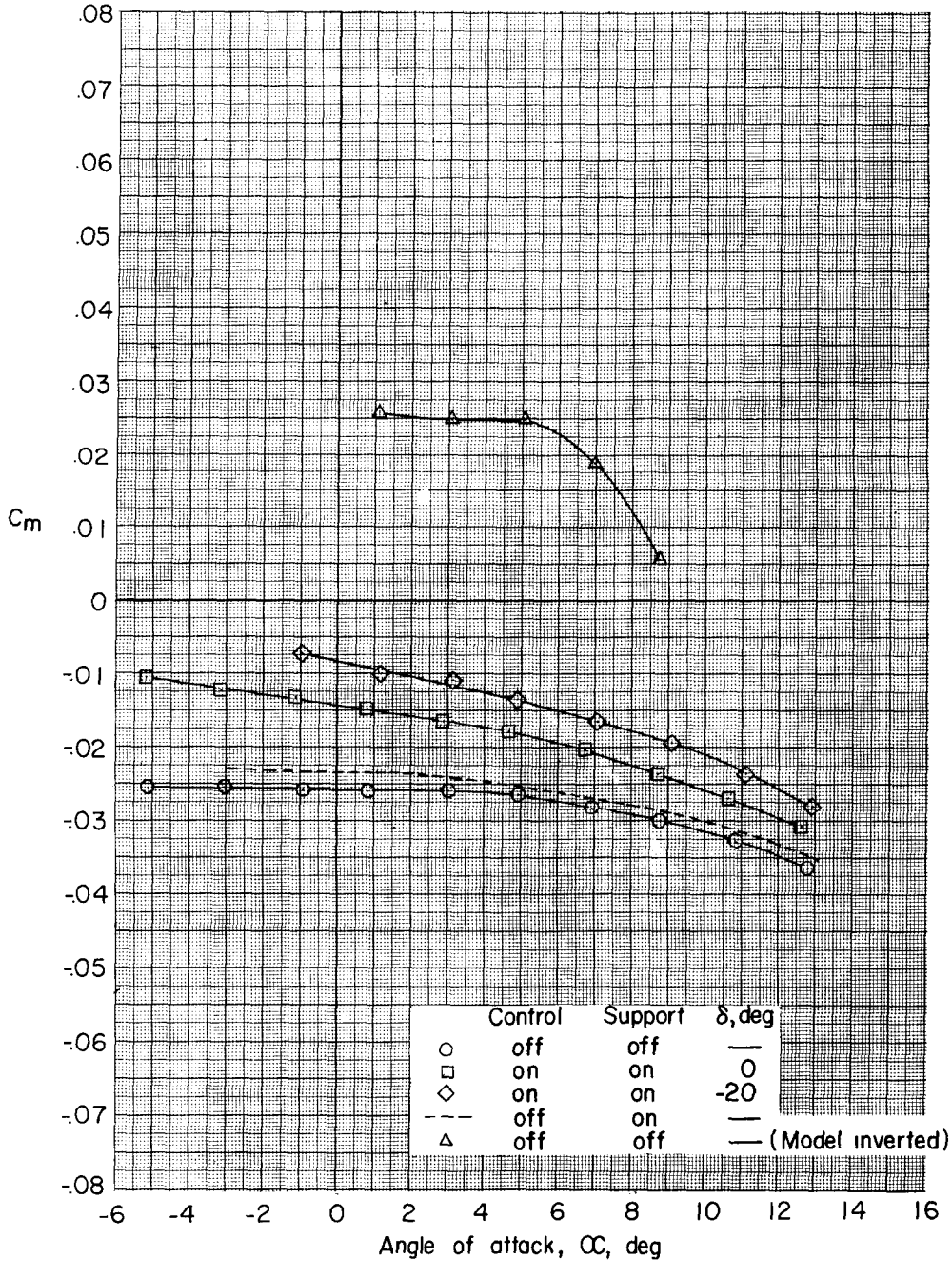

(a) Upper controls.

Figure 6.- Pitching-moment characteristics at 0° sideslip of a circular plan-form reentry vehicle with and without pyramidal controls.

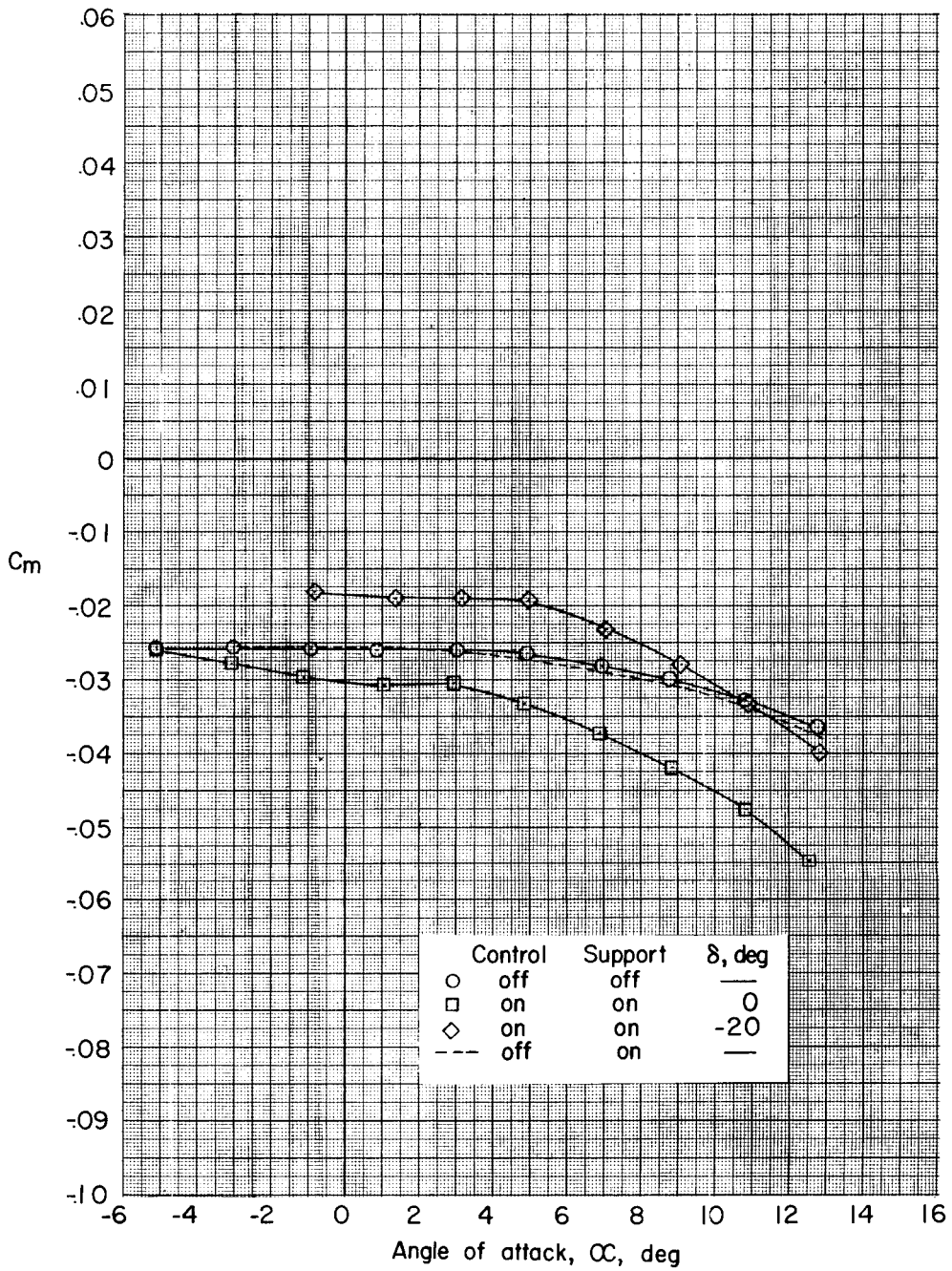

(b) Lower controls.

Figure 6.- Concluded.

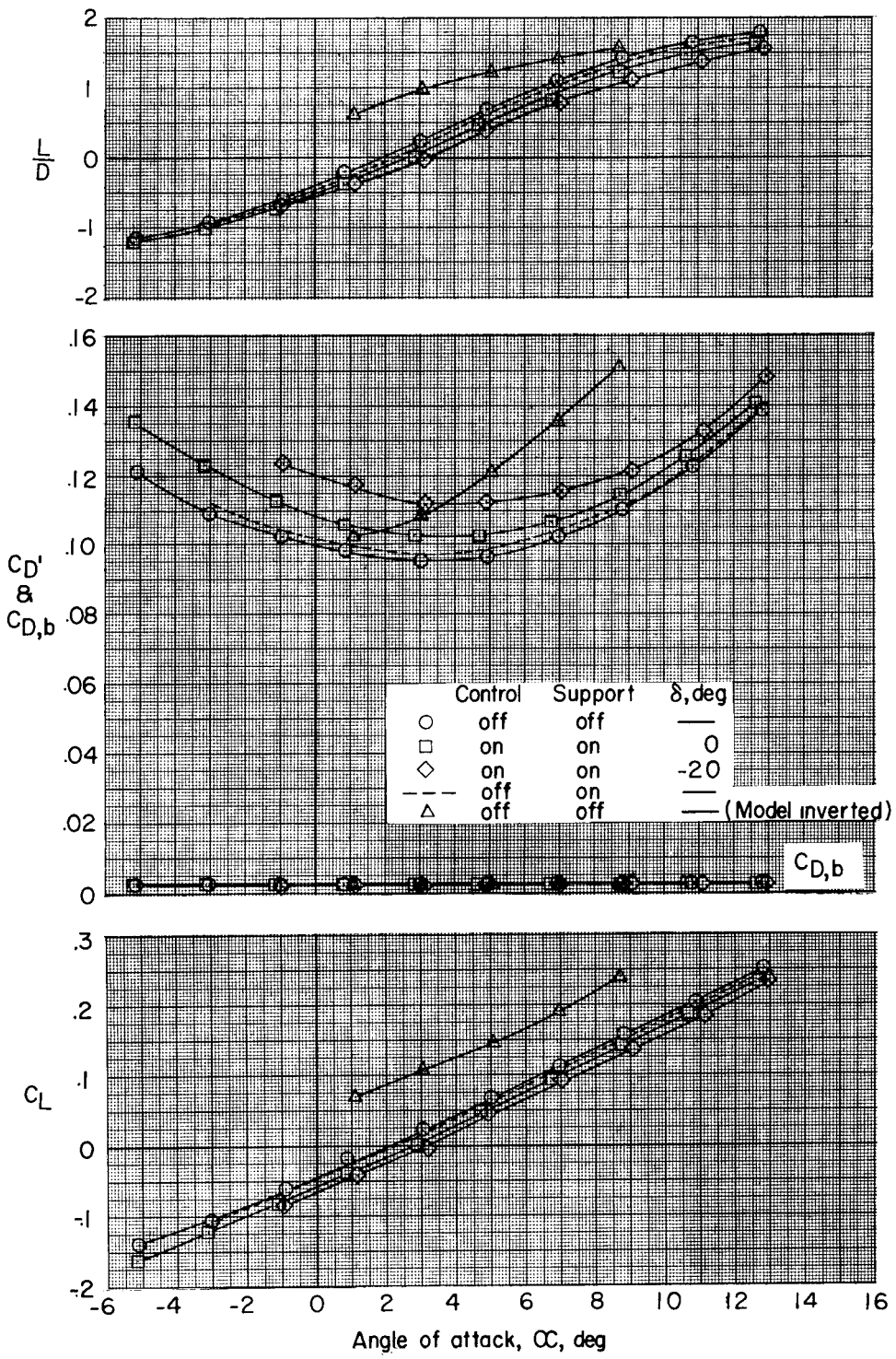

(a) Upper controls.

Figure 7.- Lift and drag characteristics at 0° sideslip of a circular plan-form reentry vehicle with and without pyramidal controls.

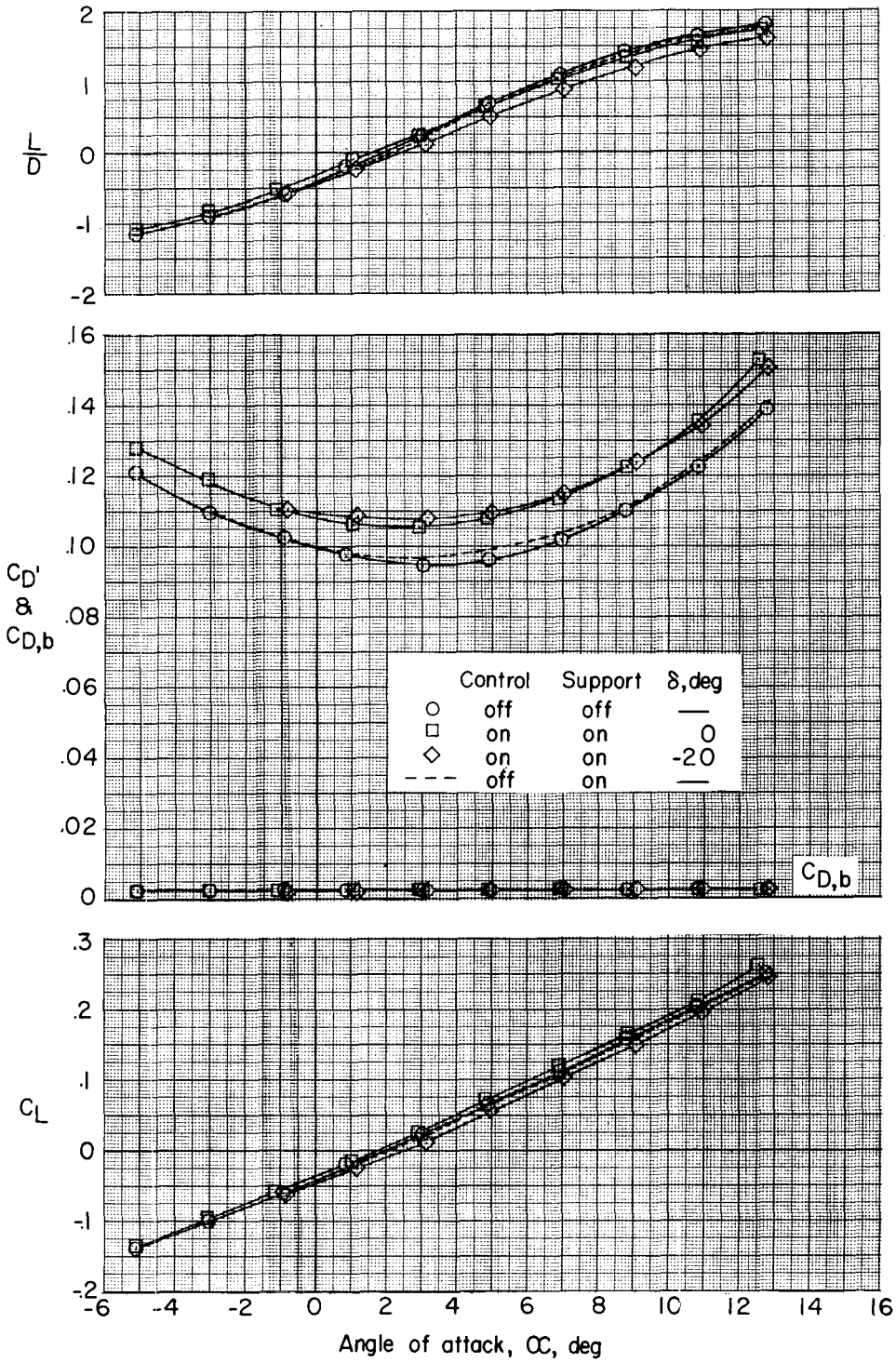

(b) Lower controls.

Figure 7.- Concluded.

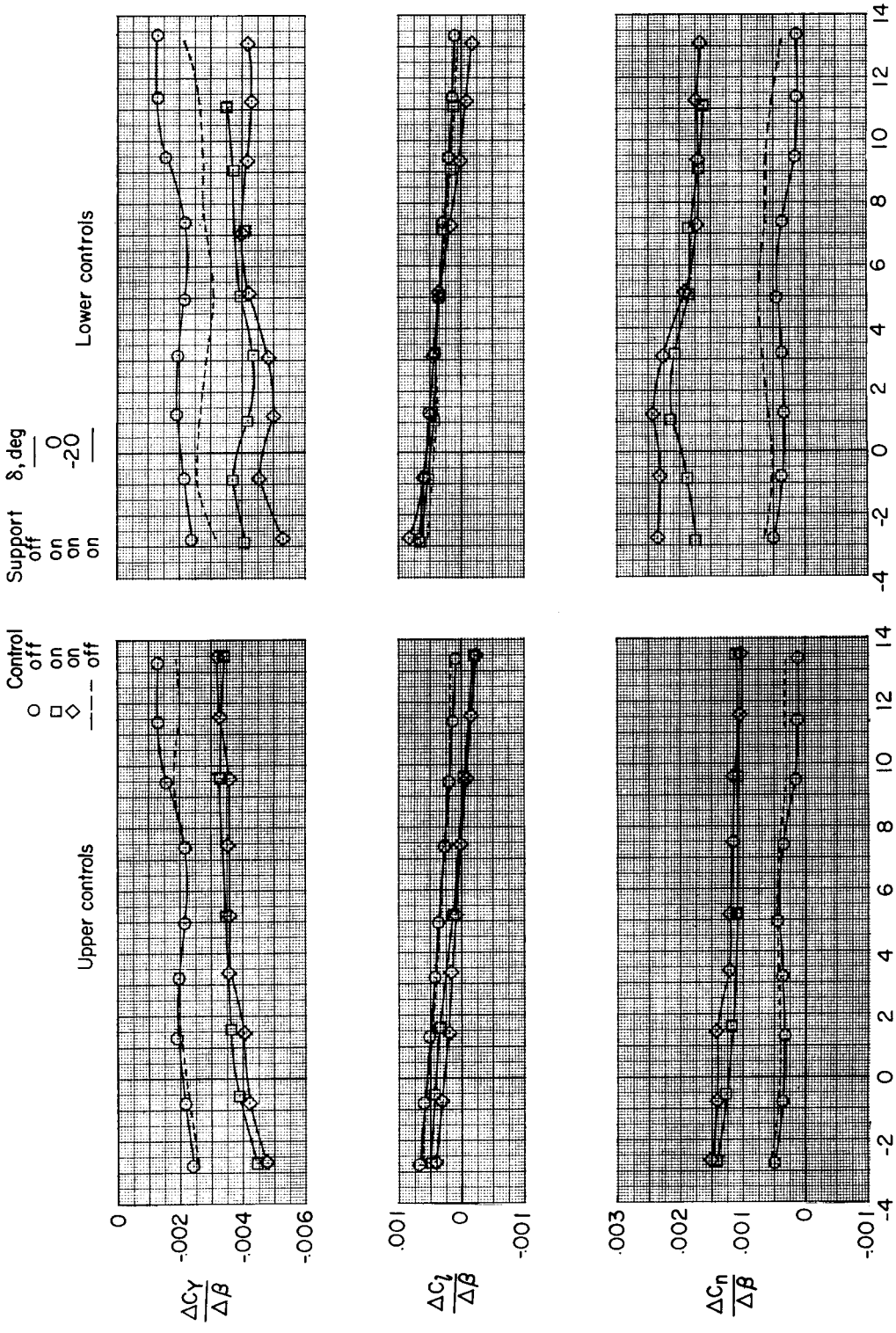

Figure 8.- Variation of $\Delta C_Y/\Delta\beta$, $\Delta C_l/\Delta\beta$, and $\Delta C_n/\Delta\beta$ with angle of attack for a circular planform reentry vehicle with and without pyramidal controls.